Characterisation of Si_3N_4 ring resonators

Bachelor Thesis

P. Wiersma
R. Amram

Laser Physics & Nonlinear Optics

Abstract

The characterisation of ring resonators has been carried out to explore the qualities of Si_3N_4 as a medium for the confinement of light. Characterising ring resonators is an important first step in using these structures for research into nonlinear optical effects (such as Raman lasing) as the extent of the usability of the structures can be predicted. Raman lasing has been measured and characterised in other materials such as silica and silicon [1][2], but either the losses are high or the nonlinear effects are hard to achieve in these materials. By using Si_3N_4 as a medium, we introduce a favourable mode profile and very low losses which yields a high quality factor. A range of Si_3N_4 ring resonators has been characterised in terms of free spectral range (FSR) and resonance width (FWHM), as such fully describing the operation of the system. Knowing the quality factor of the structure allows for a quantitative assessment of the possibilities for Raman lasing in Si_3N_4 waveguides.

Contents

Introduction

Low optical losses are generally desirable when designing waveguiding optical structures. Having low losses means that less energy is lost to absorption and scattering, allowing for more efficient operation. Also, an optical structure that presents low absorption losses will be more thermally stable, since these materials heat up less due to optical losses.
Integrated optics has become an important area of research, as well as industry. Active integrated components have been developed, but they are constructed from high-gain materials which in general absorb more light. Due to fabrication challenges, it is currently not feasible to fabricate chips using both active, high-gain, components and passive, transparent components. One solution is to use a low-gain transparent material, such as Si_3N_4, to create both active and passive components.

By using nonlinear effects, such as stimulated Raman emission, active components can be created in Si_3N_4 waveguides. These components take the form of ring resonators, which are ring-shaped waveguides, because they allow the buildup of the high intensities required for non-linear processes. In this report, a set of ring-resonators has been characterised and presented. Each of the rings is made up of a Si_3N_4 core with SiO_2 cladding on a Si wafer.

Chapter 1

Theory

1.1 Waveguides

In a waveguide light can be confined and guided. In its simplest form, it consists of two materials with different refractive indices, where the lower refractive index material (cladding) surrounds the higher refractive index material (core). If light travels through the core, it will reflect off the cladding through total internal reflection. Total internal reflection can only take place on an interface going from higher refractive index to lower refractive index[3].
The most common example of a waveguide is the optical fiber. Fibers have a cylindrical geometry, containing a glass core surrounded by cladding made of a different type of glass with a slightly lower refractive index. Since the core and cladding are very thin (typically around 1μm), they are fragile, so a protective mantle usually surrounds the cladding.
The light inside the waveguide interferes with itself after reflecting. Because of this interference process, the waveguide can only support certain sets of k-vectors. These are called modes. Each mode has its own transverse electric field distribution inside the waveguide, as caused by the interference pattern. Waveguides can be either single-mode or multi-mode, meaning they support only one mode or a variety of modes. The dimensions of the waveguide determine what modes are allowed. A bigger cross-section will support more modes.

The light in a waveguide is not completely confined to the core of the waveguide. In the vicinity of the core, an evanescent field will be present. This field decays exponentially with distance and is non-propagating. However, it can interact with nearby structures. For example, if two waveguides are placed very close to each other, light from one waveguide will leak into the other. This effect is called evanescent coupling and can be used to transfer (or couple) light from one waveguide into another. Evanescent coupling is a periodic process. Light will couple from one waveguide to another completely and the couple back into the first waveguide, because of destructive interference. The separation distance between the waveguide determines the overlapping field strength and therefore the coupling strength.

1.2 Ring Resonators

Ring resonators are ring-shaped waveguides, as can be seen in figure 1.1. Light is coupled into a ring resonator by e.g. evanescent coupling, usually by placing a straight waveguide close to the ring. To avoid destructive interference inside the ring, an integer number of the wavelength must fit inside the ring. On resonance, the light interferes constructively:

$$\lambda_{allowed} = \frac{nL}{2\pi m} \tag{1.1}$$

where L is the physical path length, n is the refractive group index, m is an integer and λ is the wavelength. Light that does not satisfy this condition will interfere destructively inside the ring. This leads to a filtering behaviour.

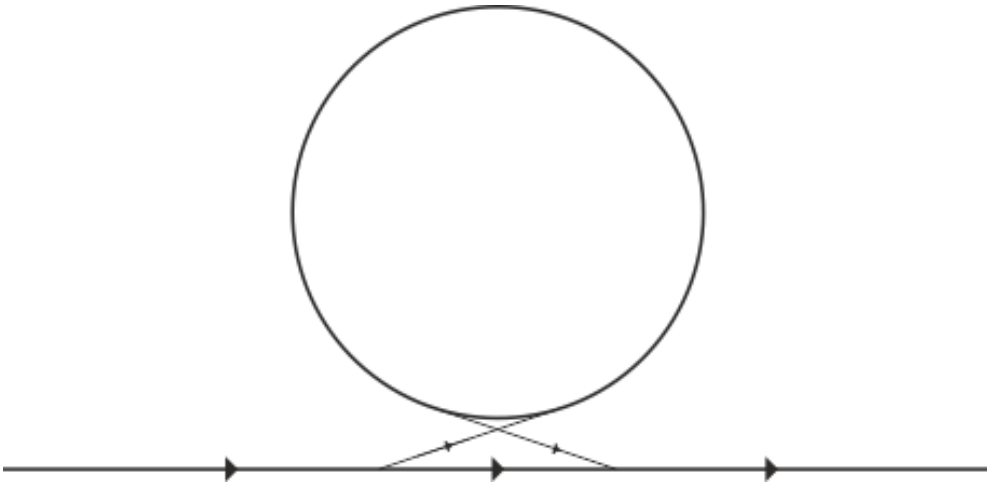

Figure 1.1: Picture of a ring resonator. The arrows indicate the transmission direction of the light. The thin lines indicate the coupling region and directions.

During each round trip, the light inside the ring experiences several types of losses. These include absorption losses, bending losses, coupling losses and scattering losses from material impurities. These losses can be incorporated in a power attenuation factor α ($\alpha = 1$ corresponds to a lossless ring).
There are three coupling regimes. Critical coupling occurs when the losses, α, equal the coupling coefficient, t, of the ring. No light is transmitted through the waveguide. Light that passes the ring is of exactly the same magnitude, but 180 degrees out of phase, as the light being coupled out of the ring, hence all the light is lost in the ring. In this case the intensity buildup of the ring is highest.
When $t < \alpha$, the ring resonator is called undercoupled. The amount of light that couples out of the ring, back into the waveguide, is not of a sufficiently high intensity to interfere completely destructively with the light that passes the ring and gets transmitted through the waveguide. Therefore the intensity in the ring is lower than in the critical coupling case.
When $t > \alpha$, the ring is called overcoupled. Light will couple out of the ring, into the waveguide. When this happens, the light makes fewer round trips inside the ring. As a result, a larger spread in wavelengths can couple into the ring.
Transmission can be characterised by a single figure of merit, its finesse (F), which is defined as

$$F = \frac{FSR}{FWHM}, \tag{1.2}$$

where FSR is the free spectral range of the ring (the spectral distance between two resonance peaks) and FWHM is the full width at half maximum of one of the peaks (the width of the peaks). Since the ring resonator is a cavity, the shape of a resonance peak is expected to be Lorentzian. The free spectral range can be calculated using:

$$FSR = \frac{\lambda^2}{n_g L}, \text{ where } n_g = n_{eff} - \lambda \frac{\partial n_{eff}}{\partial \lambda} \tag{1.3}$$

where λ is the wavelength at which the FSR is calculated, n_g is the refractive group index and L is the physical path length [4]. This formula is only valid for small dispersion, which is the case for Si_3N_4 at the relevant wavelengths [5].

In figure 1.2, the transmission goes to zero. This indicates critical coupling. If the system was undercoupled, the FWHM would not change, but the transmission would not go to zero. If the system was overcoupled, the FWHM would increase and the transmission would not go to zero.

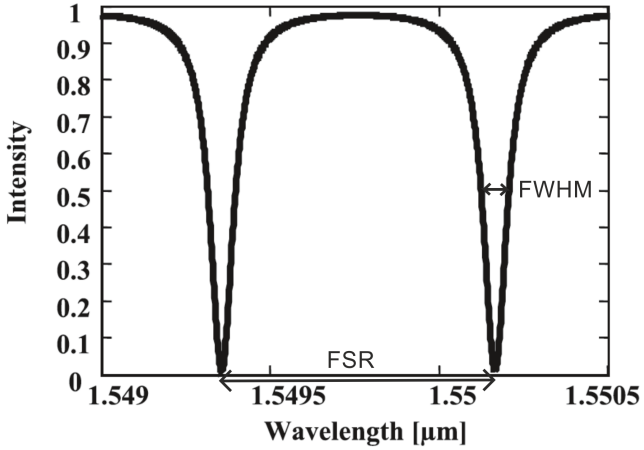

Figure 1.2: FSR and FWHM of a ring resonator.

Another important parameter of a ring resonator is the quality factor (Q-factor). It is a measure of the temporal confinement of light inside the ring resonator. It is defined as the ratio of the operating wavelength divided by the resonance width

$$Q = \frac{\lambda}{FWHM}, \tag{1.4}$$

which can be rewritten using equations 1.2 and 1.3 to

$$Q = \frac{L}{\lambda} F, \tag{1.5}$$

The Q-factor determines the minimum required duration of light coupling into the ring in order to saturate the ring. This minimum time is called the cavity buildup time τ_{cav}, and equals

$$\tau_{cav} = \frac{\lambda Q}{2\pi c_0}, \tag{1.6}$$

where c_0 is the vacuum speed of light[4]. The cavity buildup factor B is equal to

$$B = \frac{F}{\pi} \tag{1.7}$$

for low coupling coefficients between the ring and the waveguide[4].

1.2.1 Tuning the resonance of the rings

As seen from equation (1.1), it is possible to tune the resonance peaks of the ring resonator by changing the optical path length. This can be achieved by e.g. heating the rings, as they will expand and their refractive index will change. The refractive index change decreases the optical path length, while the expansion increases the physical path length. The physical path length change due to expansion is effectively larger than the optical path length change due to

refractive index change. The rings used in this research all contain gold heaters on top of part of the cladding of the ring (see fig. 1.3). By applying a voltage across a heater, a current will flow, causing resistive heating of the heater. Since the size of the heaters depends on the size of the rings, the heater resistance will vary according to ring size.

Figure 1.3: Cross-sectional schematic of part of a ring with a heater on top. The grey area is the silicon wafer. The cladding layers of SiO_3 are green. The Si_3N_4 core is blue. The yellow part on top is the gold heater.

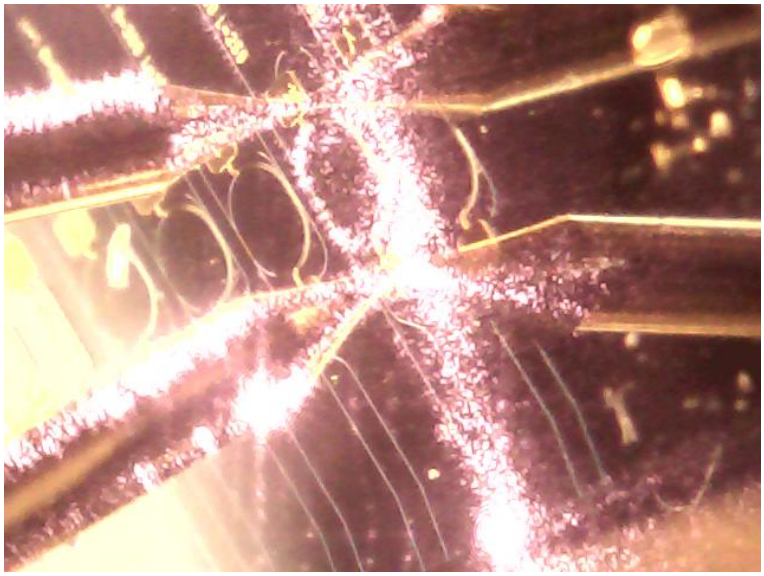

Figure 1.4: Picture of a ring brought into resonance by heating the ring. The ring is bright, as it is dissipating a lot of light. Two pens are connected to the heater pads (gold rounded squares), allowing a current to flow. Their reflections are visible in the silicon. Heaters are on the right half of each of the rings. Picture was taken with a silicon-based USB microscope. The laser used is a tunable, fiber amplified Nd:YAG laser.

Another way of heating the ring is by sending light into it. Due to absorption losses, the ring will dissipate heat when light is inside it. This causes the resonant wavelength to shift, so that the light in the waveguide will no longer enter the ring. For high power laser beams, this effect can cause problems when not properly corrected for.
The solution is to scan the laser wavelength upwards, allowing the system to reach a stable equilibrium [6]. Slowly scanning the laser wavelength upwards will cause the ring to heat up, so that its resonant wavelength will become shorter. As the scan progresses, the intensity inside the ring builds up, until the laser wavelength is equal to the resonant wavelength of the ring. At this point, the transmission through the waveguide is at a minimum. Increasing the laser wavelength any more will cause the pump to go out of resonance, decreasing the intensity and thus the absorption inside the ring, causing it to cool down which shifts the resonance wavelength downwards again, until the ring has cooled completely and is back to its initial resonance. A ring in resonance can be seen in fig. 1.4.

Chapter 2

Experimental setup and diagnostics

2.1 Goals and methods

The purpose of this assignment was to characterise Si_3N_4 ring resonators. In order to do that, several optical parameters had to be measured. Determining the intensity buildup factor, B, that can be achieved in the ring resonators is of high importance, because it is a measure of the intensity inside the rings, relative to the intensity input of the waveguides, which can be measured independently. Having a high intensity in the ring will allow a variety of nonlinear optical effects to take place, specifically third-order effects such as Raman emission and four-wave mixing. As shown in equations 1.7 and 1.2, the intensity buildup factor B can be determined by measuring the free spectral range and the bandwidth of the resonator modes of the rings.
For measuring the free spectral range, a broadband superluminescent diode (SLD) is used, in combination with an optical spectrum analyser (OSA). Unfortunately, the resolution of the OSA is not sufficiently high to determing the bandwidth of the resonator modes, so the width of the resonator modes is determined by scanning the wavelength of a spectrally narrowband laser over a resonance and measuring the FWHM of the output power as a function of the laser wavelength.

2.1.1 Coupling into the waveguide

In order to perform the previously described measurements of the ring resonators, a sufficient amount of light needs to be coupled into the input waveguide. Two ways of coupling light into the waveguide will be described here.
The easiest method is to use a fiber-coupled (so-called pigtailed) source, without additional optics. By carefully aligning the end of the fiber very close (on the order of a wavelength) to the waveguide, light will couple into it. A high-precision three-axis translation stage was used to align the fiber close to the waveguide. However, even after carefully optimizing the alignment, the coupling efficiency was measured to be quite low, on the order of a few percent. We attribute the the low coupling to poor mode matching, i.e. that the spatial shape of the light exiting the fiber does not overlap properly with the spatial shape of the waveguide. !!!REFERENCE!!! The mode field diameter of the fiber is 7.2 μm, while the mode field diameter of the waveguide is 1.5 μm for a wavelength of 1050 nm.
An alternative method is to use a microscope objective. We selected an objective with a high numerical aperture (NA) in order to generate a small focal spot. By matching the NA of the objective to the NA of the waveguide, the coupling efficiency should increase significantly, as the mode overlap with the waveguide is much better than when using a non-matched fiber. The objective should be mounted on a three-axis translation stage in order to precisely control its position. This method does require some free-space optics (lens and mirrors), as the beam has to

be collimated. Also, the objective requires the beam to enter the objective at its center and with a zero incidence angle.

2.2 The Setup

2.2.1 Free spectral range

In order to measure the free spectral range, light from an SLD is coupled into the waveguide using a fiber. The light exiting the waveguide is then collected using another fiber to guide it to an OSA for measuring its spectrum. The SLD has a center wavelength of about 1050 nm and a bandwidth of 50 nm. Depending on the optical roundtrip length of the inspected ring resonator, this measurement will show ten to a few hundred resonances superimposed on the broadband spectrum of the SLD. Measuring the spectral distance of these dips yields the free spectral range of the resonator.
The SLD is a Thorlabs SLD1050P; the OSA is an Ando AQ-6315A Optical Spectrum Analyzer. This setup is displayed in figure 2.1.

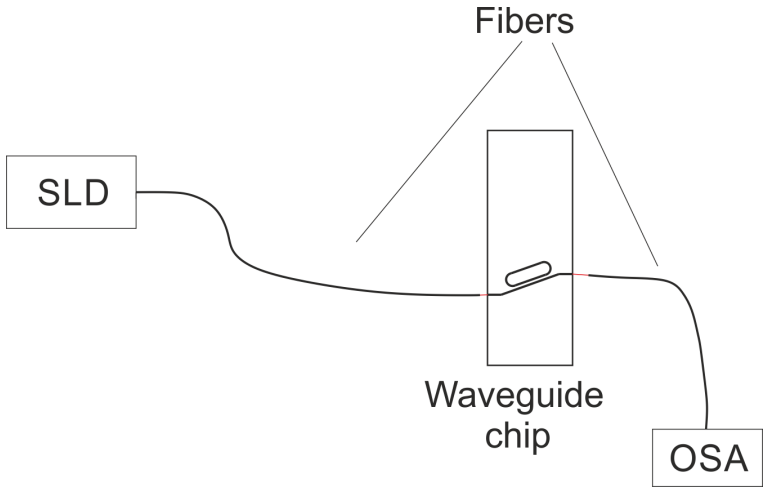

Figure 2.1: Setup for measuring FSR. The SLD used is a Thorlabs SLD1050P; the OSA is an Ando AQ-6315A Optical Spectrum Analyzer.

2.2.2 Full width at half max

In order to measure the width of a resonance dip, our initial approach was to use a fiber-coupled scanning Fabry-Pérot interferometer (FFP) (Micron optics FFP-TF2, F=350, FSR=9THz) in combination with the SLD. The FFP contains a piezo actuator to vary the distance between the mirrors and can therefore scan across a resonance. A fiber, connected to the SLD, couples light into the waveguide and the transmitted light collected on the other side of the waveguide is sent through the FFP. When scanning the FFP across a resonance, the transmitted intensity of the FFP is a convolution of the resonance and the transmission function of the FFP. After measuring the width of the convolution, the resonance width can be determined by deconvolution. The outgoing intensity is determined using an amplified silicon photodiode (PD) (Thorlabs PDA10A-EC). Unfortunately, in spite of serious experimental efforts, this method of measurement did not work. No light was transmitted through the FFP. Even when coupling the SLD directly to the FFP, any light exiting the FFP did not have a high enough intensity to show a signal above the noise level of the PD, or to show signal above noise on the OSA. A possible reason for this is that not enough light is transmitted through the FFP to be measured by the photodiode. The SLD is a broadband source, so its spectral density is very low. The FFP has a narrow transmission peak,

so almost all of the light is reflected rather than transmitted ($1/F\%$ of the light). This setup is displayed in figure 2.2.

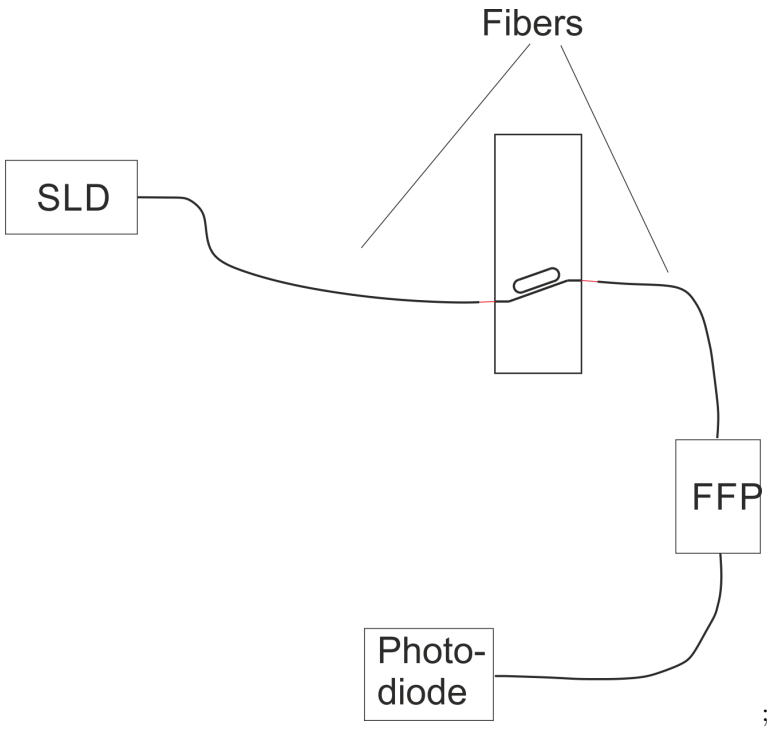

;

Figure 2.2: Setup for measuring FWHM. The SLD used is a Thorlabs SLD1050P; the FFP is a (Micron optics FFP-TF2, F=350, FSR=9THz); the PD is a Thorlabs PDA10A-EC.

A second method that was attempted for measuring the FWHM is tuning a narrowband continuous wave (CW) laser. The laser that we selected is a tunable fiber-amplified Nd:YAG laser operating at a wavelength of 1064 nm. The tuning range of the laser is about 0.06 nm. The light is coupled into the waveguide using a microscope objective. The microscope objective has an NA of 0.65 and a magnification of 40X. The resonance of the ring is tuned, as described in section 1.2.1, because of the limited tuning of the laser. First, It is tuned to a minimum transmission, which is the center of the resonance dip. Then the laser wavelength is scanned in a controlled manner across the resonance. The power of the light is recorded using the OSA. An OSA was used rather than a photodiode, because the OSA measures over a wavelength range, showing when the laser mode-hops. This setup is displayed in figure 2.3.

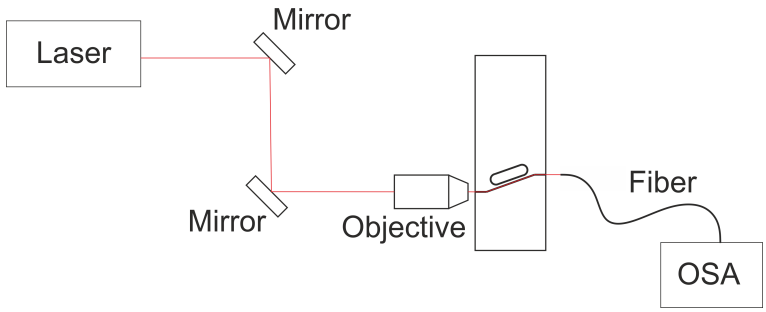

Figure 2.3: Improved setup for measuring FWHM. The laser is a tunable fiber-amplified Nd:YAG laser at 1064 nm; the OSA is an Ando AQ-6315A Optical Spectrum Analyzer; the objective has an NA of 0.65 and a magnification of 40X.

2.3 Measurements

Three rings are going to be characterised. Their geometries are different from the simple ring resonator geometry shown in figure 1.1. They are racetrack-shaped; two half-circles with straight sections in between. The input/output waveguide is aligned with one of these straight sections, allowing coupling over a longer length which increases the coupling coefficient between the ring and the waveguide. In addition to the input-output waveguide, some of the rings also contain a drop-port waveguide. This is a waveguide which couples to the other side of the ring, where it can accept light coming from the ring, as shown in figure 2.4.

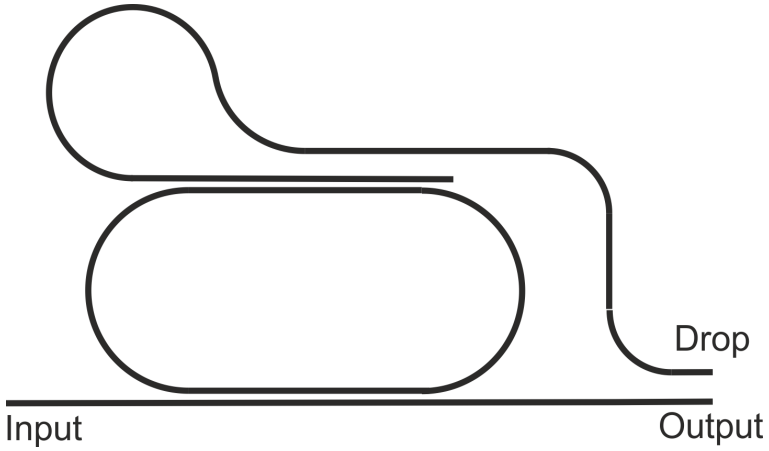

Figure 2.4: Geometry of used ring resonators.

The drop port does not influence the measurements of the FSR or the FWHM. The specifications of the rings are

Ring #	Coupling length (μm)	Radius (μm)	Calculated FSR (nm)
1	100	50	1.29
2	250	50	0.82
3	300	250	0.31

Table 2.1: Specifications of characterised rings. The FSR of the rings in table 2.1 is calculated using equation (1.3).

Chapter 3

Results

A brief overview of the specifications of the ring resonator structures.

3.1 Free spectral range

The free spectral range of each of the rings in table 2.1 has been determined, using the methods described in section 2.2.1. In figure 3.1, part of the transmission spectrum of ring 1 is shown. This is a typical spectrum for these measurements. Part of the spectrum of the light exiting the drop port of the first ring is shown in 3.2. As expected, the dips in the transmission are seen as peaks in the drop port.

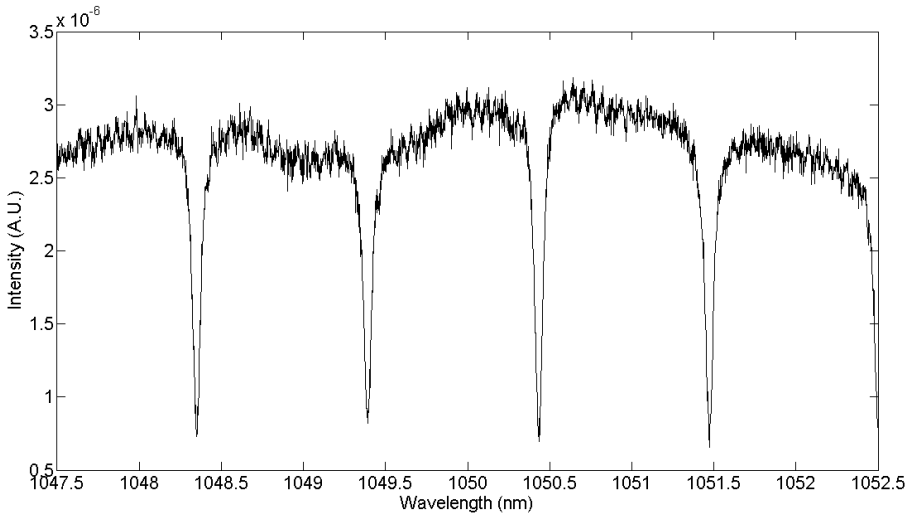

Figure 3.1: Transmission spectrum of the light exiting ring 1. The light source is an SLD. The spectrum has been recorded using an OSA.

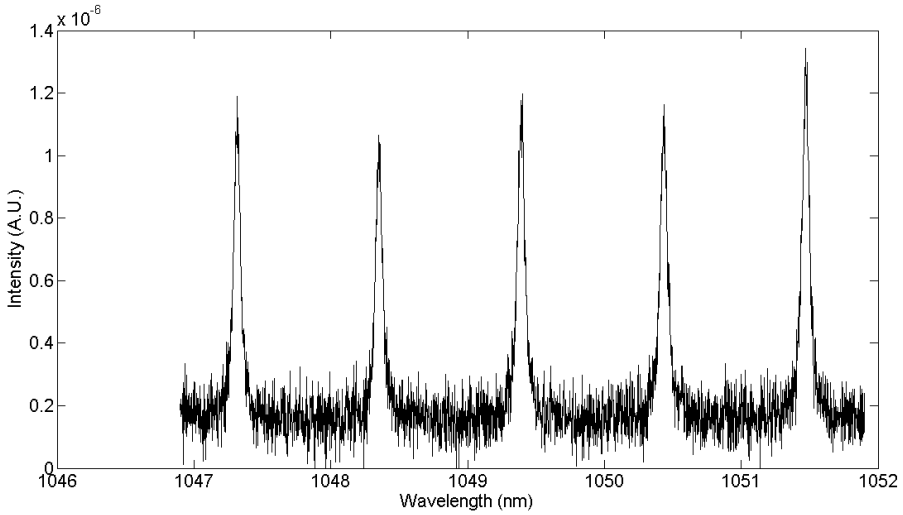

Figure 3.2: Spectrum of the drop port of the light exiting ring 1.

In table 3.1, the measured FSR of each of the three rings is given.

Ring #	Coupling length (μm)	Radius (μm)	Calculated FSR (nm)	Measured FSR (nm)
1	100	50	1.29	1.04
2	250	50	0.82	0.65
3	300	250	0.31	0.24

Table 3.1: Measurements of the FSR of the rings.

3.2 Full width half max

The FWHM of rings 2 and 3 in table 2.1 has been determined, using the methods described in section 2.2.2. In figures 3.3 and 3.4, resonance dips can be observed.

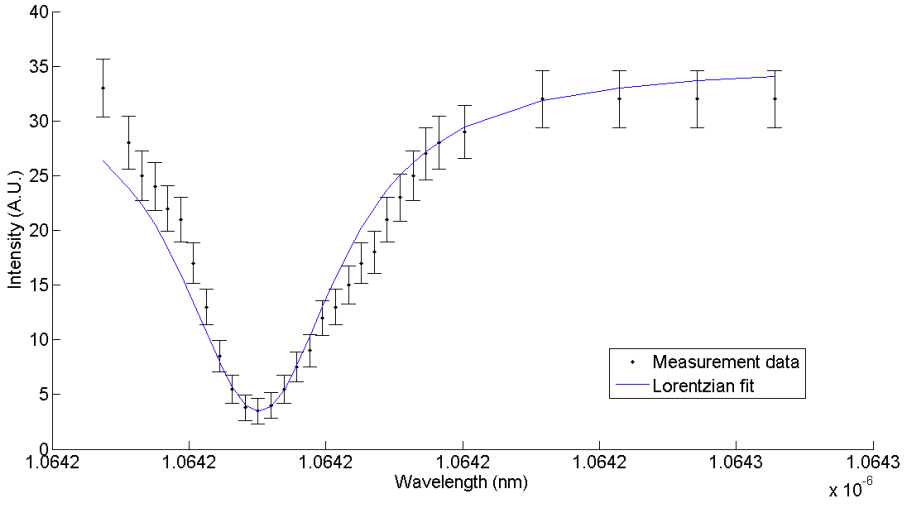

Figure 3.3: Resonance dip of ring 2.

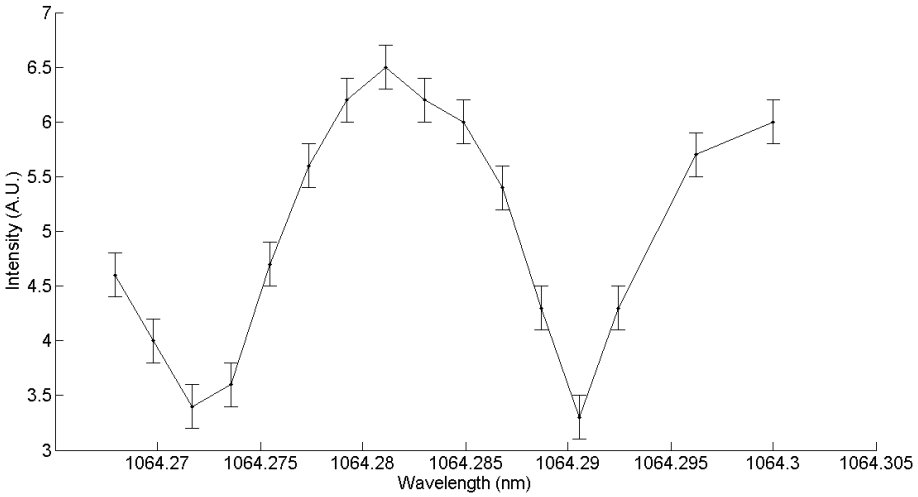

Figure 3.4: Resonance dip of ring 3.

In figure 3.3, a Lorentzian function has been fitted to the results. In figure 3.4, the double dip prevented such a fitting method, so the FWHM has been determined manually. The double dip is likely caused by a higher order mode, which has a slightly different effective refractive index.

Ring #	Measured FSR (nm)	Measured FWHM (nm)	Finesse	Q-factor	Buildup
2	0.65	0.014	45.9	69800	14.6
3	0.24	0.035	6.9	10400	2.2

Table 3.2: Results.

Discussion and Conclusion

The goal of the experiment was to develop a method for measuring the quality of ring resonators. This has been achieved by measuring the spectral distance between resonances (FSR) and by measuring the spectral width of a resonance. The measured values of the FSR consistently differ from the calculated values by about 25%. This can be explained by a variety of factors. However, we expect that this discrepancy occurs because the exact n_{eff} is not known. The finite element calculations that were performed to determine the value for n_{eff} showed rather different values for small material and optical differences. The thermal effects, as described in section 1.2.1, have been observed at high laser powers (>100mw). These effects have not been observed during the characterisation process, as the low laser power used did not yield enough absorption losses to significantly heat the ring.

Our results suggest that if light can be coupled into the waveguide efficiently, it should be possible to observe nonlinear effects in the resonators.

Bibliography

[1] S. M. Spillane, T. J. Kippenberg, and K. J. Vahala, "Ultralow-threshold raman laser using a spherical dielectric microcavity," Nature **415** (2002).

[2] O. Boyraz and B. Jalali, "Demonstration of a silicon raman laser," Optics Express **12** (2004).

[3] F. L. Pedrotti, L. M. Pedrotti, and L. S. Pedrotti, *Introduction to Optics* (Pearson, 2007), 3rd ed.

[4] D. G. Rabus, *Integrated ring resonators* (Springer, 2007).

[5] "Refractive index database," `http://refractiveindex.info/?group=CRYSTALS&material=Si3N4`. Accessed: 2013-07-05.

[6] T. Carmon, L. Yang, and K. J. Vahala, "Dynamical thermal behavior and thermal self-stability of microcavities," Optics Express **12** (2004).